中国光学工程学会会刊

ISSN 1007-2276
CN 12-1261/TN

第48卷 | 第4期
Vol.48 | No.4

2019.04

# 红外与激光工程

# INFRARED AND LASER ENGINEERING

★ 图片来源： Terahertz radiations of a butterfly-shaped photoconductive antenna/Jitao Zhang

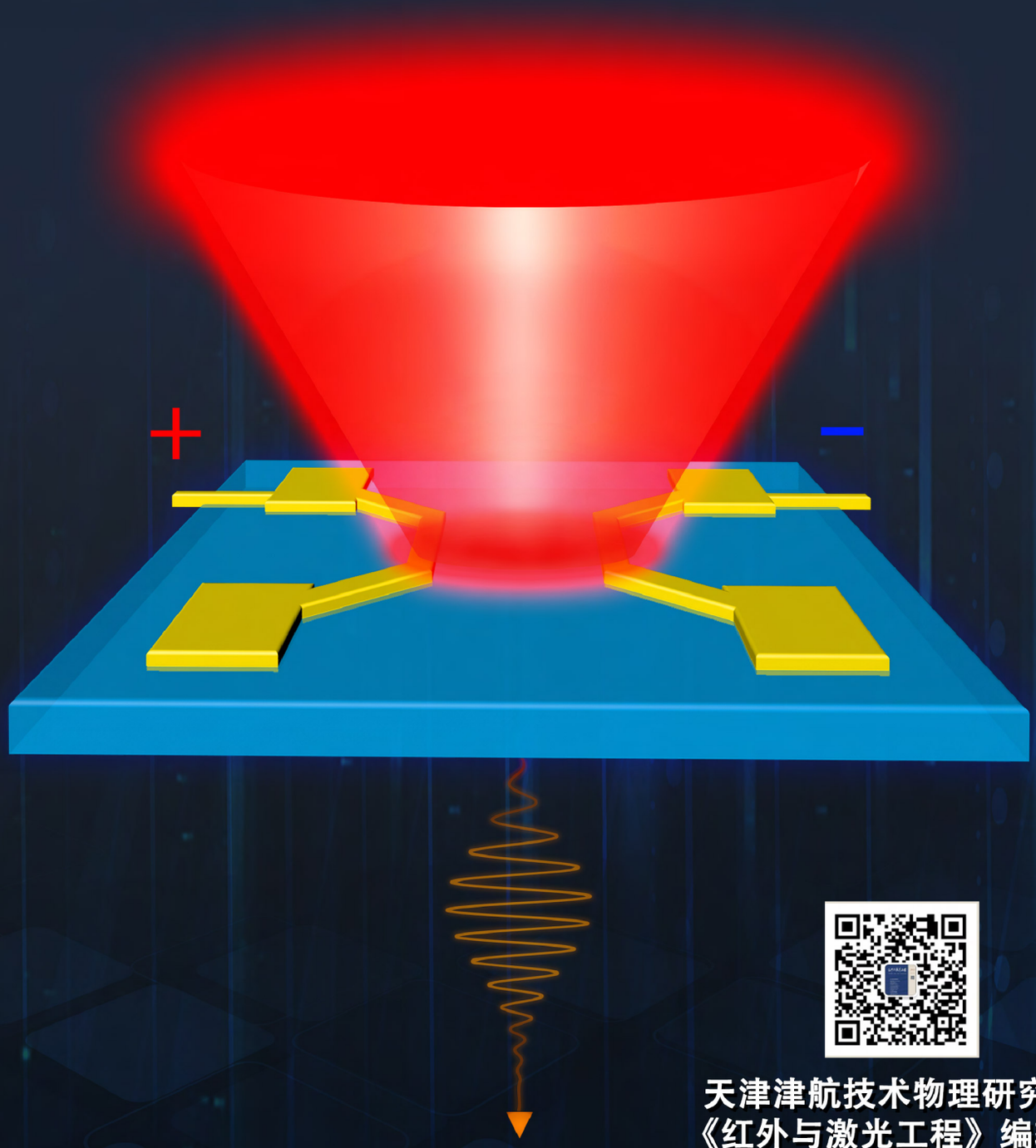


天津津航技术物理研究所
《红外与激光工程》编辑部

# Terahertz radiation of a butterfly-shaped photoconductive antenna(invited)

Jitao Zhang[1,2], Mingguang Tuo[1], Min Liang[1], Wei-Ren Ng[1], Michael E. Gehm[1,3], Hao Xin[1]

(1. Department of Electrical and Computer Engineering, University of Arizona, Tucson, AZ, 85721 USA;
2. Fischell Department of Bioengineering, University of Maryland, College Park, Maryland, 20742 USA;
3. Department of Electrical and Computer Engineering, Duke University, Durham, NC, 27708 USA)

**Abstract:** The terahertz(THz) far-field radiation properties of a butterfly-shaped photoconductive antenna (PCA) were experimentally studied using a home-built THz time-domain spectroscopy(THz-TDS) setup. To distinguish the contribution of in-gap photocurrent and antenna structure to far-field radiation, polarization-dependent THz field was measured and quantified as the illuminating laser beam moved along the bias field within the gap region of electrodes. The result suggests that, although the far-field THz radiation originates from the in-gap photocurrent, the antenna structure of butterfly-shaped PCA dominates the overall THz radiation. In addition, to explore the impact of photoconductive material, radiation properties of butterfly-shaped PCAs fabricated on both low-temperature-grown GaAs (LT-GaAs) and semi-insulating GaAs (Si-GaAs) were characterized and compared. Consistent with previous experiments, it is observed that while Si-GaAs-based PCA can emit higher THz field than LT-GaAs-based PCA at low laser power, it would saturate more severely as laser power increased and eventually be surpassed by LT-GaAs-based PCA. Beyond that, it is found the severe saturation effect of Si-GaAs was due to the longer carrier lifetime and higher carrier mobility, which was confirmed by the numerical simulation.

**Key words:** terahertz; photoconductive antenna; butterfly; time domain spectroscopy

**CLC number:** TN821$^{+}$.4 **Document code:** A **DOI:** 10.3788/IRLA201948.0402001

Received date: 2018-11-14; Revised date: 2018-12-28

Foundation item: National Science Foundation(1126572)

Author: Jitao Zhang(1985-), male, Assistant Research Professor, Doctor. His research is focused on optics and precision instrumentattion, including optical interferometry, terahertz antenna and spectroscopy, and Brillouin microscopy. Email: zhangjt06@gmail.com

## 0 Introduction

Along with the development of terahertz (THz) technology since 1980s[1], photoconductive antenna (PCA) has been one of the most commonly used THz sources due to its simple configuration and broadband spectra. One of the representative applications of PCAs is the THz time-domain spectroscopy (THz-TDS), where the PCA is used as a THz emitter and/or detector[2-3]. A typical PCA consists of the photoconductive material as substrate and the antenna structure deposited on top, which together determines the radiation properties. As a ultrafast laser pulse hits the photoconductive material of a externally biased PCA, a photo-excited current will be generated within the illuminated gap region of the PCA and part of them will flow to the antenna structure. According to the Maxwell′s equations, any transient current will result in electromagnetic radiation. As to the PCA, both the photo-excited current in the gap and the portion that flows to the antenna structure contribute to the overall THz radiation. Although massive efforts have been done to explore the THz radiation properties of PCAs fabricated with different photoconductive materials and antenna structure[4-13], the universal understanding of the radiation mechanism of the PCA remains unclear[4], and one of the central questions is how to distinguish the contribution of in-gap photocurrent and antenna structure to the overall THz radiation. In this work, our effort is devoted to address this question by experimentally studying the radiation properties of a butterfly-shaped PCA, a new antenna structure that is rarely explored before. Different from the bowtie PCA which has a spectral band of a few THz[4], a butterfly-shaped PCA (Fig.1) has four symmetrically-distributed extensions (named as "wings") starting from the ends of a coplanar stripline. The overall length of wings is about millimeter to obtain optimized THz radiation at sub-THz regime (0.025-0.4 THz), and the coplanar stripline in the center region ensures a quick and easy alignment of the illuminating laser beam.

Here, we propose a method to identify the contribution from in-gap photocurrent and antenna structure using butterfly-shaped PCA. By moving the laser beam spot within the gap region along the direction of biased field, less photocurrent can flow to the antenna structure due to the limited carrier lifetime of the carriers; thus the THz radiation from the antenna structure will decrease. Whereas the radiation from the in-gap photocurrent will not be affected. In case the beam spot is far enough from the electrode so that none photo-excited carrier can reach the electrode before recombination, the THz radiation will be solely from the in-gap photocurrent. Therefore, by monitoring the overall radiation of a PCA against the position of the laser beam, the radiation portion of in-gap photocurrent and antenna structure can be quantified. With the above methodology, we found the antenna structure dominates the overall THz radiation of the butterfly-shaped PCA, while the contributes of the in-gap photocurrent is much less but cannot be ignored. This is consistent with the numerical simulation based on 3D full-wave model[14]. In addition, we studied the impact of photoconductive materials on the radiation properties. We found that although Si-GaAs-based PCA can emit higher THz field than LT-GaAs-based PCA at low laser power, it would saturate much earlier as the laser power increased and eventually be surpassed by LT-GaAs-based PCA. This is consistent with previous experiment where different antenna structures were used[4]. Furthermore, we explored that the more severe saturation effect of Si-GaAs was due to the

longer carrier lifetime and higher carrier mobility, which was confirmed by the numerical simulation.

## 1 PCA fabrication and experiment setup

The size of the whole antenna chip is 2 mm× 2 mm (Fig.1(a)). The central region of the PCA is a coplanar stripline with a length of 100 μm, a line-width of 5 μm, and a gap size of 34 μm (Fig.1 (b)). Four wings are connected to the ends of the stripline symmetrically. The LT-GaAs-based PCA is commercially fabricated on a 650 μm thick Si-GaAs substrate with a 3 μm LT-GaAs epi-layer on top and 0.2 μm AlAs as the heat-spreader layer in between. A $SiO_2$ passivation layer is deposited on top of the central antenna region to improve the optical transmission. The Si-GaAs based PCA is in-house fabricated on a 360 μm thick Si-GaAs substrate, which is <100> oriented, and has a carrier concentration of $1.37\times10^7$ $cm^{-3}$ and dark resistivity of $9.1\times10^7$ Ω·cm. The electrodes are made of 20 nm Cr/150 nm Au by standard photolithography and lift-off techniques.

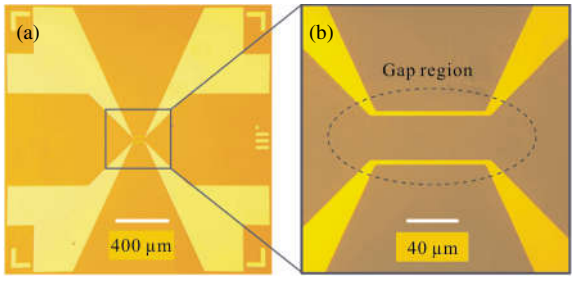


Fig.1 Microscopic image of an in-house fabricated butterfly-shaped stripline PCA on Si-GaAs substrate with 5 μm stripline line-width. The zoomed-in image shows the central region of the PCA and the dashed arrow within the antenna gap indicates the direction of the external bias field

To efficiently couple the THz radiation into free space, the PCA chip is carefully attached onto the center of a hyper-hemispherical silicon lens to maintain the polarization. Figure 2 shows the schematic of the experimental THz-TDS system setup. The PCAs under study are used as the THz emitter. A commercial butterfly-shaped PCA with a 6 μm gap dipole structure in the central region (model: PCA-44-06-10-800-h, BATOP GmbH) is used as the THz detector,

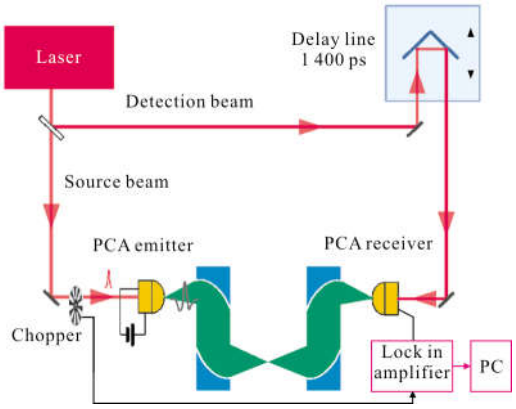


Fig.2 Schematic of the experimental THz-TDS system setup

which is also integrated with a hyper-hemispherical silicon lens. A Ti:sapphire fs laser (Micra 5, Coherent Inc.) with a center wavelength of 800 nm and a repetition rate of 80 MHz is used as the optical source to pump and gate the emitter and detector, respectively. The laser beam with an approximate spot size of 20 μm is focused into the gap of the emitter and located close to the anode to optimize the THz radiation field. Four off-axis parabolic mirrors are used to guide and reshape the THz beam. A linear translation stage is used to generate a time delay between the optical pump and probe beam paths. The photocurrent of the detector is pre-amplified by a trans-impedance amplifier (not shown in the schematic) before being detected by a lock-in amplifier (SR850, Stanford Research Systems). A mechanical chopper is inserted in the pump beam path to improve the signal-to-noise ratio of the detected signal.

## 2 Results and discussion

### 2.1 Polarization-dependent THz radiation

The in-gap photocurrent only excites vertically

polarized ($x$–axis) THz radiation, which is parallel to the direction of the external bias field (Fig.3). In contrast, the polarization of THz radiation from the electrode depends on its structure. Ideally, the horizontal–polarized ($y$–axis) THz radiation will be cancelled out due to symmetry. In practice context, however, the radiation from antenna structure of the butterfly–shaped PCA consists of both horizontal and vertical components, due to the imperfect positioning of the laser beam in $x$–axis.

The contributions of the photocurrents both in the gap and on the antenna structure were quantified by measuring the dependence of the THz field polarization on the laser beam location. The PCA receiver is only sensitive to $y$–component of THz field because the central gap region has a dipole shape. By placing PCA emitter in different orientation, the radiation components at different directions can be measured. The PCA under test was measured in the parallel configuration(Fig.3(a)) and perpendicular configuration(Fig.3(b)). For each case, the focused laser spot is scanned along the direction from the anode toward the cathode (as indicated by the "+" and " – " signs) by a translational stage, and the corresponding THz signals are recorded.

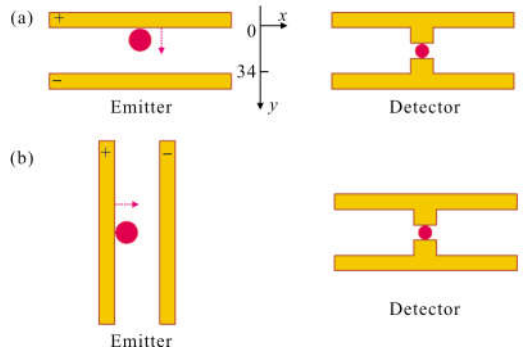


Fig.3 Arrangement of the PCAs for polarization–dependent measurement. Only the central regions of the butterfly–shaped PCAs are shown for simplicity. (a) Parallel configuration, (b) perpendicular configuration, where the PCA emitter is rotated by 90 degree. The dashed arrow indicates the moving direction of laser beam

A butterfly–shaped PCA fabricated with LT–GaAs was used as the emitter and the diameter of the focused laser spot was approximately 20 μm. The scanning step of the laser spot was 4 μm. The results are shown in Fig.4. We first notice that the THz field in parallel configuration is larger than that in perpendicular configuration, regardless of the spot po sition. This indicates that the THz

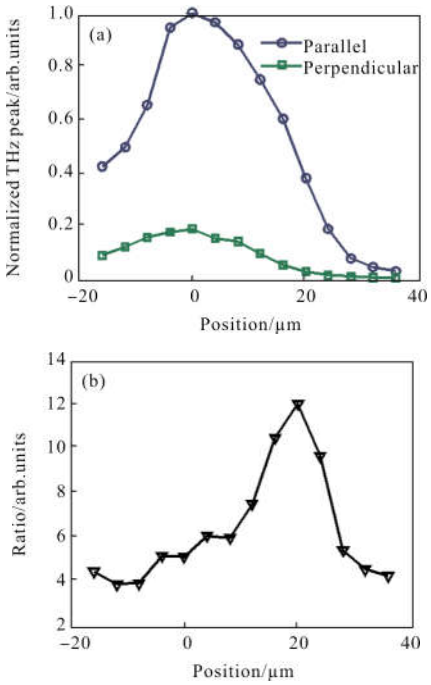


Fig.4 Polarization dependence of the THz field of the PCA on the laser spot location. (a) Normalized peak values of the detected THz fields by the same detector with respect to the laser spot location when the PCA emitter is arranged in the parallel (blue open circle) and perpendicular (green open square) configurations, (b) ratio of the parallel to perpendicular curves in (a)

radiation parallel to the bias field ($y$–axis) is always dominant. We also observe that the THz signal is the strongest when the laser spot is in the vicinity of the anode in both configurations, which is consistent with previous observations[15–16]. Since the receiver is only sensitive to the vertical–polarized component ($y$–axis) of the incoming THz field, the detected signal in the perpendicular configuration indicates that there is still fair amount of THz radiation polarized in the $y$–direction. This is a result of the symmetry

breaking, which is due to the position offset of the laser spot along the *y*–direction in experiment.

Figure 4(a) clearly shows the THz radiation strongly depends on the location of the laser spot. When the laser spot is close to the anode, a lot of photo–excited electrons (holes are ignored due to much smaller mobility) could flow to the electrode before recombination and contribute to the THz radiation. When the laser spot is moved away from the anode, the contribution of the current on the electrode will decrease because less electrons can arrive at the electrode. As shown in Fig.4(b), the ratio of two polarized components increases as the laser spot is moved away from the anode. This is expected because both polarization components of THz radiation from antenna structure decrease while the component (*x*–axis) of THz radiation from in–gap photocurrent remains unchanged. The ratio is maximum as the laser spot is approximately 20 μm away from the initial position. In this case, the radiation field solely from the electrode has dropped by approximately 84%, according to the perpendicular case in Fig.4 (a). However, the radiation in the parallel configuration only drops by approximately 62%. Because the decreased radiation can be only from the anode electrode, we deduce that when the laser beam is in the vicinity of the anode, the portion of the THz radiation from the current on the electrode and within the antenna gap are about 74% and 26%, respectively (Appendix A). This suggests that the radiation from antenna structure dominates the overall radiation of butterfly–shaped PCA. Further moving the beam spot results in the decreasing of the photo–excited current and thus the THz field because the laser beam is partially blocked by the cathode.

### 2.2 Effect of photoconductive materials

Figure 5 shows the measured time–domain THz signals and the corresponding spectra of two identical PCAs fabricated on LT–GaAs and Si–GaAs substrates. The signals were acquired in the parallel configuration. The duration of the time–domain main pulse is approximately 8 ps. The measured peak frequency of both PCAs is around 0.05 THz and the spectrum span is about 1 THz. In this context, the Si–GaAs based PCA has slightly higher THz radiated field compared to the LT–GaAs based PCA. In addition, the LT–GaAs–based PCA exhibits a shorter pulse width (thus a bit broader THz bandwidth) than the Si–GaAs–based PCA due to its shorter carrier lifetime.

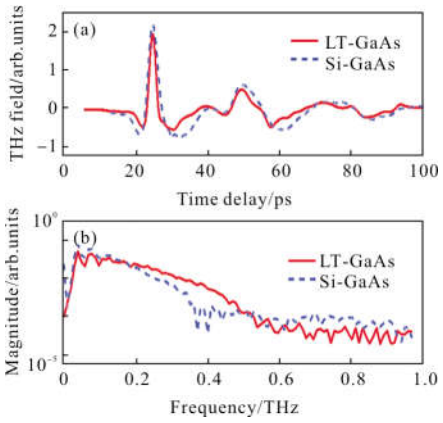


Fig.5 Time– and frequency–domain plots of the measured THz far–field radiation emitted by the Si–GaAs–based (blue dashed curve) and the LT–GaAs–based (red solid curve) PCAs. Both have identical butterfly shape. The data are collected under the same pump laser power of 10 mW and DC bias voltage of 25 V

The dependencies of the THz peak field on biased voltage and pump laser power for the two PCAs are shown in Figs.6 and 7, respectively. In Fig.6, the biased voltage was swept from 1 to 25 V with a 2–V increment at several laser power level (i.e., 2 mW, 6 mW, 10 mW, and 14 mW). The THz peak field emitted by the LT–GaAs–based PCA increases almost linearly with regards to the biased voltage. In contrast, the response of the Si–GaAs based PCA shows a nonlinear trend, which increases rapidly at low voltage but saturates quickly at high voltage. In addition, both PCAs have similar radiation field at initial voltage (i.e.,

<7 V) but the LT-GaAs based PCA is outperformed by the Si-GaAs-based PCA with higher voltage (i.e.,>10 V) under moderate laser excitation. However, the difference becomes smaller as the laser power increases due to the quick saturation of Si-GaAs-based PCA. The saturation effect is closely studied in Fig.7, where the same dataset of Fig.6 are redrawn in a way that the pump laser power is swept at the same DC bias voltages. In Fig.7, the

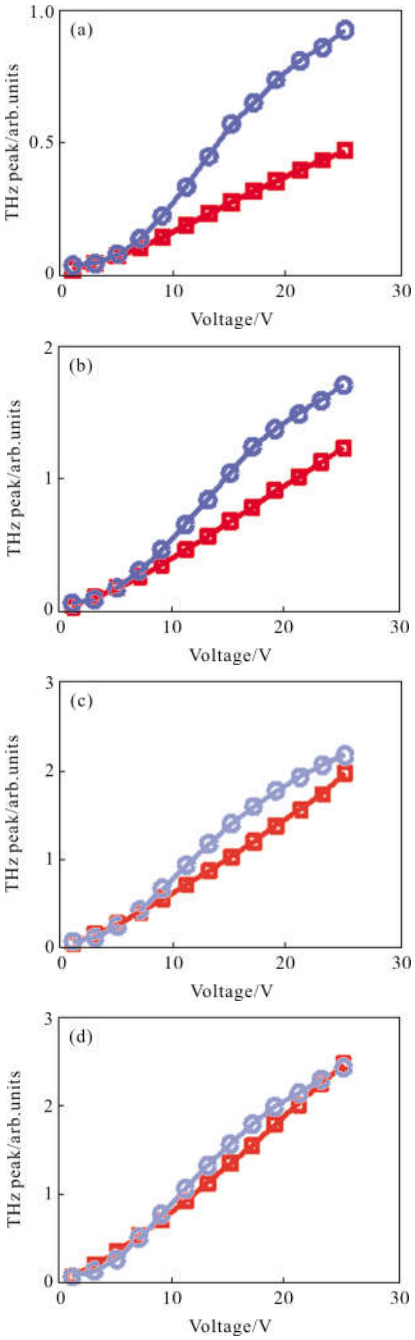


Fig.6 Dependence of THz peak fields of the Si-GaAs-based (blue open circle) and the LT-GaAs-based (red open square) PCAs on DC bias voltage under the laser power level of (a) 2 mW, (b) 6 mW, (c) 10 mW, and (d) 14 mW. The solid lines are a guide of eye

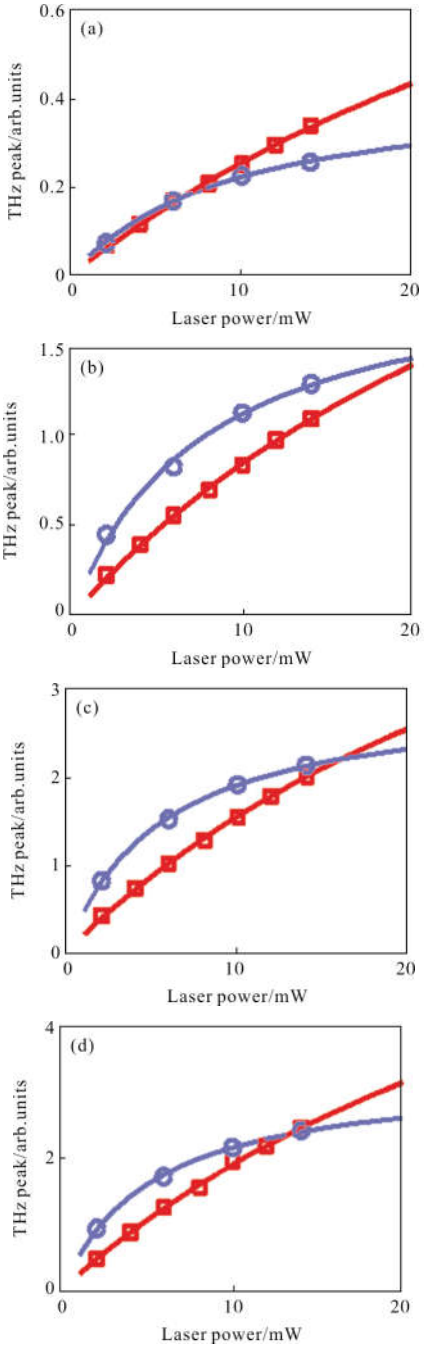


Fig.7 Dependence of THz peak fields of the Si-GaAs-based (blue open circle) and the LT-GaAs-based (red open square) PCAs on laser power at DC bias voltage level of (a) 5 V, (b) 13 V, (c) 21 V, and (d) 25 V, with the same dataset of Fig.6. The solid lines are the fitted curves of the measured data according to the scaling rule[13, 15]

experimental data are fitted by Eq.(1) according to the scaling rule[15,17]:

$$E_{\mathrm{THz}}=D\frac{P}{P_0+P} \tag{1}$$

where $E_{\mathrm{THz}}$ is the THz field; $P$ is the laser power; $D$ and $P_0$ are fitted coefficients related to the properties of the laser and photoconductive substrate. As shown in Fig.7, both PCAs show saturation effect with regard to the pump laser power, but the Si-GaAs-based PCA saturates at a lower laser power. This is a result of the screening effect that has been observed before[4]. However, the underlying mechanism that drive the Si-GaAs to saturate more severely is unclear.

According to Eq.(1), larger carrier mobility of Si-GaAs would result in smaller $P_0$[14] and the screening effect caused by the space charges would further deplete the bias filed, which ultimately makes the saturation effect of the Si-GaAs-based PCA more severe than that of the LT-GaAs-based PCA. In addition, the fitted curves in Fig.7 indicate that the radiated THz field of the Si-GaAs-based PCA would ultimately be surpassed by the LT-GaAs-based PCA under high laser power.

To verify that the more severe saturation effect of Si-GaAs is due to the long carrier lifetime and high mobility, numerical 3D full-wave model simulations was implemented by homemade Matlab program[18-20] to study the laser power dependence of the PCAs based on the LT-GaAs and Si-GaAs substrates[21]. In this simulation, the carrier dynamics of the semiconductor are coupled with Maxwell equations, so that the THz far-field radiation of the PCA can be predicted directly. The electron carrier lifetimes of LT-GaAs and Si-GaAs are 0.1 ps and 10 ps, respectively. The electron mobilities of LT-GaAs and Si-GaAs are 600 $cm^2/(V\cdot s)$ and 5 000 $cm^2/(V\cdot s)$, respectively. The laser beam has a diameter of 20 μm and is located near the anode of the PCA. The simulated PCA has a typical stripline structure featuring a pair of parallel straight strips. The strips have a gap of 34 μm, a line-width of 5 μm and a line-length of 50 μm. The antenna is biased at 20 V. The total simulation volume is 50 μm×44 μm×2.2 μm. The simulation results in Fig.8 indicates that LT-GaAs-based PCA will surpass Si-GaAs-based PCA at higher pump laser power, which shows similar trend as the experimental observation in Fig.7.

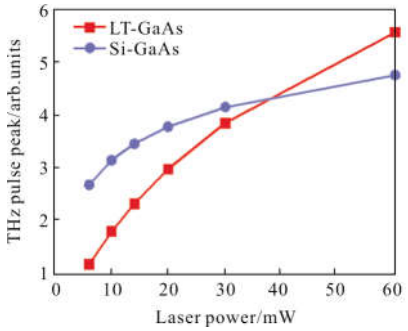


Fig.8 Simulation results of a typical stripline antenna to verify the saturation effect in Fig.7. The solid squares and circles represent the THz peak fields of the time-domain pulse under each laser pump power with a DC bias of 20 V for LT-GaAs and Si-GaAs, respectively. The solid lines are a guide of eye

## 3 Conclusion

The THz radiation properties of a butterfly-shaped PCAs are characterized using a home-built THz-TDS system. It is validated that the dominant THz radiation of this PCA comes from the photocurrent on the antenna structure, while the radiation from in-gap photocurrent is much less but cannot be ignored. In addition, the effect of photoconductive material was explored with LT-GaAs and Si-GaAs substrates. Consistent with previous experiment, we found that both SI-GaAs and LT-GaAs-based PCA shows saturation effect as the laser power increases, and the Si-GaAs-based PCA saturates faster. Beyond that, we found the more severe saturation effect of Si-GaAs was

due to the longer carrier lifetime and higher carrier mobility, which was confirmed by numerical simulation.

## Appendix A

Suppose radiation contribution of the photo-excited currents within the antenna gap and on the electrode is $\left(0, I_{g0}^{V}\right)$ and $\left(I_{e0}^{H}, I_{e0}^{V}\right)$, respectively, when the laser spot is in the vicinity of the anode. The components in the brackets indicate the horizontal -and vertical -polarized components. Thus in the parallel configuration

$$I_{g0}^{V}+I_{e0}^{V}=1 \tag{a1}$$

When the laser beam is 20 μm away from the initial position, $I_{g0}^{V}$ does not change while both $I_{e0}^{H}$ and $I_{e0}^{V}$ decrease by 84%. In addition, the overall radiation in the parallel configuration drops by 62%. Similar to Eq.(a1), one can get

$$I_{g0}^{V}+(1-0.84)I_{e0}^{V}=1-0.62 \tag{a2}$$

By solving Eqs. (a1) and (a2) together, one can get $I_{g0}^{V}$ and $I_{e0}^{V}$ are 26% and 74%, respectively.

### References:

[1] Auston D H, Cheung K P, Smith P R. Picosecond photoconducting Hertzian dipoles [J]. ***Applied Physics Letters***, 1984, 45(3): 284-286.

[2] Jepsen P U, Cooke D G, Koch M. Terahertz spectroscopy and imaging -Modern techniques and applications [J]. ***Laser & Photonics Reviews***, 2011, 5 (1): 124-166.

[3 Burford N M, El-Shenawee M O. Review of terahertz photoconductive antenna technology [J]. ***Optical Engineering***, 2017, 56(1): 010901.

[4] Tani M, Matsuura S, Sakai K, et al. Emission characteristics of photoconductive antennas based on low -temperature -grown GaAs and semi -insulating GaAs [J]. ***Applied Optics***, 1997, 36(30): 7853-7859.

[5] Jepsen P U, Jacobsen R H, Keiding S R. Generation and detection of terahertz pulses from biased semiconductor antennas [J]. ***Journal of the Optical Society of America B***, 1996, 13(11): 2424-2436.

[6] Tani M, Yamamoto K, Estacio E S, et al. Photoconductive emission and detection of terahertz pulsed radiation using semiconductors and semiconductor devices [J]. ***Journal of Infrared, Millimeter, and Terahertz Waves***, 2012, 33(4): 393-404.

[7] Hou L, Shi W. An LT-GaAs terahertz photoconductive antenna with high emission power, low noise, and good stability [J]. ***IEEE Transactions on Electron Devices***, 2013, 60(5): 1619-1624.

[8] Reklaitis A. Comparison of efficiencies of GaAs-based pulsed terahertz emitters [J]. ***Journal of Applied Physics***, 2007, 101: 116104.

[9] Miyamaru F, Saito Y, Yamamoto K, et al. Dependence of emission of terahertz radiation on geometrical parameters of dipole photoconductive antennas [J]. ***Applied Physics Letters***, 2010, 96(21): 211104.

[10] Gao Y, Yang C E, Chang Y, et al. Terahertz-radiation-enhanced broadband terahertz generation from large aperture photoconductive antenna [J]. ***Applied Physics B***, 2012, 109(1): 133-136.

[11] Liu T A, Chou R H, Pan C L. Dependence of terahertz radiation on gap sizes of biased multi-energy arsenic-ion-implanted and semi-insulating GaAs antennas [J]. ***Applied Physics B***, 2010, 95(4): 739-744.

[12] Kono S, Gu P, Tani M, et al. Temperature dependence of terahertz radiation from n-type InSb and n-type InAs surfaces [J]. ***Applied Physics B***, 2000, 71(6): 901-904.

[13] Zhang J, Mikulics M, Adam R, et al. Generation of THz transients by photoexcited single-crystal GaAs meso-structures [J]. ***Applied Physics B***, 2013, 113(3): 339-344.

[14] Zhang J, Tuo M, Liang M, et al. Contribution assessment of antenna structure and in -gap photocurrent in terahertz radiation of photoconductive antenna [J]. ***J App Phys***, 2018, 124: 053107.

[15] Darrow J T, Zhang X C, Auston D H, et al. Saturation properties of large-aperture photoconducting antennas [J]. ***IEEE Journal of Quantum Electronics***, 1992, 28 (6): 1607-1616.

[16] Keil U D, Dykaar D R. Ultrafast pulse generation in photoconductive switches [J]. ***IEEE Journal of Quantum Electronics***, 1996, 32(9): 1664-1671.

[17] Benicewicz P K, Taylor A J. Scaling of terahertz radiation from large-aperture biased InP photoconductors [J]. ***Optics Letters***, 1993, 18(16): 1332-1334.

[18] Sano E, Shibata T. Fullwave analysis of picosecond photoconductive switches [J]. ***IEEE Journal of Quantum Electronics***, 1990, 26(2): 372-377.

[19] Moreno E, Pantoja M F, Garcia S G, et al. Time-domain numerical modeling of THz photoconductive antennas [J]. ***IEEE Transactions on Terahertz Science and Technology***, 2014, 4(4): 490-500.

[20] Zhang J, Tuo M, Liang M, et al. Numerical analysis of terahertz generation characteristics of photoconductive antenna [C]//IEEE Antennas and Propagation Society International Symposium (APSURSI), 2014: 1746-1747.

[21] Zhang J. Numerical analysis of the emission properties of terahertz photoconductive antenna by finite-difference-time-domain method [J]. ***arXiv Preprint arXiv***, 2014, 1407.2881: 1-11.